The Vesicle-inducing Protein 1 from *Synechocystis* sp. PCC 6803 Organizes into Diverse Higher-Ordered Ring Structures

Eva Fuhrmann,*† Jelle B. Bultema,‡ Uwe Kahmann,§ Eva Rupprecht,* Egbert J. Boekema,‡ and Dirk Schneider*

*Institut für Biochemie und Molekularbiologie, ZBMZ, †Fakultät für Biologie, Albert-Ludwigs-Universität, 79104 Freiburg, Germany; ‡Groningen Biomolecular Sciences and Biotechnology Institute, University of Groningen, 9747 AG Groningen, The Netherlands; and §Fakultät für Biologie, Universität Bielefeld, D-33501 Bielefeld, Germany

The vesicle-inducing protein in plastids 1 (Vipp1) was found to be involved in thylakoid membrane formation in chloroplasts and cyanobacteria. In contrast to chloroplasts, it has been suggested that in cyanobacteria the protein is only tightly associated with the cytoplasmic membrane. In the present study we analyze and describe the subcellular localization and the oligomeric organization of Vipp1 from the cyanobacterium *Synechocystis* PCC 6803. Vipp1 forms stable dimers and higher-ordered oligomers in the cytoplasm as well as at both the cytoplasmic and thylakoid membrane. Vipp1 oligomers are organized in ring structures with a variable diameter of 25–33 nm and corresponding calculated molecular masses of ~1.6–2.2 MDa. Six different types of rings were found with an unusual 12–17-fold symmetrical conformation. The simultaneous existence of multiple types of rings is very unusual and suggests a special function of Vipp1. Involvement of diverse ring structures in vesicle formation is suggested.

INTRODUCTION

Structural and functional studies of the thylakoid (photosynthetic) membranes of both cyanobacteria and chloroplasts revealed many of their exclusive features. However, the biogenesis and formation of thylakoid membranes is incompletely understood today. Chloroplast thylakoid membranes evolve from vesicles originating from the chloroplast inner envelope membrane, and the formation of thylakoids results in the generation of a completely separated internal membrane system (Vothknecht and Westhoff, 2001). In contrast, for cyanobacteria it has been a long-standing debate if the internal thylakoid membrane system is physically separated or if it remains connected to the cytoplasmic membrane. Several recent structural studies have, however, indicated that thylakoids are also separated membrane entities in cyanobacteria (Liberton *et al.*, 2006; van de Meene *et al.*, 2006; Nevo *et al.*, 2007; Schneider *et al.*, 2007).

For biogenesis of thylakoid membranes many cellular processes, like lipid biosynthesis, membrane formation, protein synthesis in the cytoplasm and/or at a membrane, protein transport, protein translocation, and protein folding have to be organized, chronologically aligned, and

controlled. Although for many years genes and proteins specifically involved in formation and biogenesis of thylakoid membranes remained unidentified, in 2001 a protein was described that could be involved in thylakoid membrane biogenesis in plant chloroplasts and cyanobacteria (Kroll *et al.*, 2001; Westphal *et al.*, 2001). The observation that deletion of the open reading frame *hcf155* in *Arabidopsis thaliana* resulted in a complete absence of thylakoid membranes indicated that the encoded protein is involved in thylakoid membrane biogenesis. Further analysis has suggested that the protein might be involved in vesicle trafficking between the inner envelope and thylakoid membranes of chloroplasts (Kroll *et al.*, 2001). Consequently, the protein was named vesicle-inducing protein in plastids 1 (Vipp1). Depletion of Vipp1 in the cyanobacterium *Synechocystis* PCC 6803 strongly affected the ability of cyanobacterial cells to form thylakoid membranes (Westphal *et al.*, 2001) and consequently, also in cyanobacteria Vipp1 appears to be involved in thylakoid membrane formation. A Vipp1 depletion strain of *A. thaliana* is deficient in photosynthesis, and the defects appeared to be caused by dysfunction of the entire photosynthetic electron transfer chain (Aseeva *et al.*, 2007). On depletion of Vipp1 in cells of the cyanobacterium *Synechocystis* sp. PCC 6803 a decrease in paired thylakoid membranes has been observed together with a significant reduction of active trimeric photosystem 1 centers (Fuhrmann *et al.*, 2009). Although chloroplast Vipp1 was found to be localized in both the thylakoid and inner envelope membrane (Li *et al.*, 1994; Kroll *et al.*, 2001), the cyanobacterial protein has been suggested to be exclusively bound to the cytoplasmic membrane (Westphal *et al.*, 2001).

Vipp1 shows a high degree of sequence similarity to the phage shock protein A (PspA) from *Escherichia coli* and other

eubacteria, and—in line with this—Vipp1 can functionally replace PspA in *E. coli* (DeLisa *et al.,* 2004). The low-resolution structure of the *E. coli* PspA has been resolved by electron microscopy (EM) and single-particle analysis (Hankamer *et al.,* 2004). The homooligomeric PspA organizes into a ring structure with ninefold rotational symmetry and a molecular mass of ~1 MDa. Formation of ring structures has also been suggested for Vipp1 from *A. thaliana* (Aseeva *et al.,* 2004). However, the oligomeric organization and structure of both PspA and Vipp1 has been challenged recently. Vipp1 from the green alga *Chlamydomonas reinhardtii* forms very long rod-like structures in vitro, and a function of these structures in vivo has been suggested (Liu *et al.,* 2007). Furthermore, it has been suggested that PspA from *E. coli* forms cage-like structures that mimic eukaryotic clathrin coats (Standar *et al.,* 2008), rather than ring structures. These contradicting structural data make further studies relevant.

Here we present a detailed analysis of the oligomeric organization of Vipp1 from the cyanobacterium *Synechocystis* PCC 6803. Vipp1 forms stable dimers and higher-ordered oligomers that are localized in the cytoplasm and at the internal membranes. The higher-ordered oligomeric Vipp1 species have a molecular mass of ~1.9 ± 0.3 MDa and are organized in ring structures with a remarkably variable number of monomer copies. They might be involved in vesicle formation by a yet unknown mechanism.

MATERIALS AND METHODS

Heterologous Expression and Purification of Vipp1 from Synechocystis sp. PCC 6803

Generation of the plasmid pRSET-SynVipp1 expressing Vipp1 with an N-terminal deca His-tag is described in detail in Fuhrmann *et al.* (2009). For protein expression the expression plasmid was transformed into *E. coli* BL21 (DE3) cells. Cells were grown in 1 L LB medium to an OD_{600} of ~0.6, and protein expression was induced by addition of 0.5 mM isopropyl-beta-D-thiogalactopyranoside. After 3 h cells were harvested and resuspended in 20 ml 50 mM Na phosphate, pH 7.6, and 5 mM EDTA buffer. Cells were subsequently broken by sonication, and afterward cell debris and inclusion bodies were removed by centrifugation at 10, 000 × *g* for 10 min. The remaining supernatant was directly used to purify Vipp1. The supernatant was loaded onto a Ni-NTA agarose column (Qiagen, Hilden, Germany). The column was washed five times with buffer (50 mM Na phosphate, 300 mM NaCl, and 40 mM imidazole), and proteins were finally eluted in buffer + 500 mM imidazole. The eluted protein was subsequently dialyzed against 50 mM Na phosphate, pH 7.6.

For determination of the subcellular protein localization in *E. coli*, the supernatant retained after removal of debris and inclusion bodies was centrifuged for 1 h at 100,000 × *g*, and sedimented membranes were redissolved in buffer and brought to the same volume as the soluble protein fraction. Equal volumes of the fractions were loaded per lane for the SDS-PAGE analysis.

Synechocystis Cell Culture

A glucose tolerant *Synechocystis* sp. PCC 6803 wild-type strain (kind gift of M. Rögner, Bochum, Germany) was grown photoautotrophically in liquid BG11 medium (Rippka *et al.,* 1979) at 34°C under 33 $\mu E/m^2$ of fluorescent cold white light or under light-activated heterotrophic growth conditions (Anderson and McIntosh, 1991).

Preparation of Cyanobacterial Membranes

Synechocystis cells were harvested in the midlog growth phase and pelleted by centrifugation (5000 × *g*, 10 min, 4°C). Cells were resuspended in buffer (20 mM HEPES/KOH, pH 7.5, 150 mM NaCl, 5 mM $MgCl_2$, and 5 mM $CaCl_2$) and disrupted in a bead beater homogenizer (BioSpec, Bartlesville, OK) using 0.5-mm glass beads. Glass beads, unbroken cells, and cell debris were removed by centrifugation at 5000 × *g* for 5 min at 4°C. After subsequent centrifugation at 100,000 × *g* for 40 min at 4°C the membrane pellet was resuspended in a buffer at a chlorophyll concentration of ~1 mg chlorophyll/ml, and thylakoid membranes were extracted with 1.5% *n*-dodecyl-β-D-maltoside (DDM) for 1 h at room temperature. Proteins and protein complexes of the soluble fraction as well as extracted membrane proteins were separated on a Biosept S4000 SEC column (Phenomenex, Aschaffenburg, Germany) in

buffer (20 mM HEPES/KOH, pH 7.5, 150 mM NaCl, 5 mM $MgCl_2$, 5 mM $CaCl_2$, and 0.04% DDM). Individual fractions were analyzed by immunoblot analysis using an anti-Vipp1 antibody (Fuhrmann *et al.,* 2009) to identify Vipp1-containing fractions.

For blue native (BN) PAGE analysis freshly prepared *Synechocystis* membranes in buffer (50 mM HEPES/KOH, pH 7.0, 5 mM MgCl2, 25 mM CaCl2, and 10% glycerol) were extracted with 1.5% DDM, and membrane-attached proteins were separated exactly as described in detail in Dühring *et al.* (2006). Individual lanes were separated in a second dimension on a 12% SDS-gel (Laemmli, 1970), and Vipp1 was identified by immunoblot analysis using an anti-Vipp1 antibody.

Electron Microscopy

Synechocystis PCC 6803 cells were grown and harvested as described above. A cell pellet obtained from a 10-ml cell suspension was washed three times with EM buffer (50 mM KH_2PO_4/Na_2HPO_4, pH 7.0). The ultrastructural and immunocytochemical (immunogold) investigations were performed as described previously (Gathmann *et al.,* 2008).

On purification Vipp1 was dialyzed against 20 mM Tris/HCl, pH 7.5, 75 mM NaSCN, and 50 mM NaCl. Samples of purified Vipp1 were negatively stained with 2% uranyl acetate (UA) or 4% methylamine tungstate (MT) on glow-discharged carbon-coated copper grids. Images were recorded with a Gatan 4K slow-scan charge-coupled device camera (Pleasanton, CA) on a Philips CM12 electron microscope (FEI, Eindhoven, The Netherlands) equipped with a LaB6 tip operated at 120 kV, using Grace software for semiautomated specimen selection and data acquisition (Oostergetel *et al.,* 1998). The final magnification was ×80,000, with a pixel size (after binning the images) of 3.75 Å at the specimen level.

About 1400 electron micrographs were recorded from a specimen stained with MT. In total 13,943 single-particle projections representing top views were selected and extracted from 1402 electron micrographs, recorded from an MT-stained specimen, by a reference-based automated particle selection procedure incorporated in GRIP (Groningen Image Processing) from these micrographs. From the UA-stained specimen, 600 electron micrographs were recorded, and 625 single particles of side views were selected and extracted by hand.

Single-particle analysis was performed with the GRIP software package on a PC cluster. The single-particle projections (144 × 144-pixel frame for the top views and 160 × 160-pixel frame for the double-ring side views) were subjected to multireference alignment and reference-free alignment procedure, multivariate statistical analysis, and hierarchical ascendant classification (van Heel *et al.,* 2000). Finally, two-dimensional projection maps of Vipp1 top views were calculated from the best resolved classes, which represented ~15% of the whole data. For the final two-dimensional projection maps of the Vipp1 side views, all (80% of the) selected single particles were used to calculate averages from the best resolved classes.

To validate the imposed symmetry, cross-correlation factors (CCFs) between a nonrotated projection map and rotated views of the same projection map were calculated. The rotation angles were such chosen that they correspond to certain symmetry (a rotation of 180° corresponds to twofold symmetry, 120° rotation to threefold symmetry, etc.). Symmetry was identified based on the highest CCF score and the smallest rotation angle because structures with, for example, 12-fold symmetry also show two-, three-, four-, and sixfold symmetry.

Circular Dichroism Measurements

The secondary structure of Vipp1 was determined by circular dichroism (CD) spectroscopy. CD spectra were measured with an Jasco J-810 CD spectrometer (Jasco, Tokyo, Japan) in the 190–350-nm range every 1 nm at a scan speed of 200 nm min^{-1} in a cuvette with a 1-mm path length at a protein concentration of 0.125 mg/ml in 10 mM Na phosphate buffer (pH 7.5). The bandwidth was set to 1 nm.

GALLEX Analyses of the In Vivo Oligomerization in E. coli

The GALLEX system was used to determine homotypic interactions of Vipp1 in *E. coli*. Therefore, the *vipp1* gene was amplified by PCR from genomic *Synechocystis* DNA using the following primers: vipp3′-GALLEX: 5′-tatgcgagctcgatgggattatttgaccgtttagand-3′ and vipp5′: 5′-tatgccatatgggattatttgaccgtttagg-3′, and the resulting *vipp1* fragment was subsequently ligated to the plasmid pLexA (Schneider and Engelman, 2003) after restriction digestion of the PCR fragment and the plasmid with SacI and BamHI.

E. coli SU101 cells (Dmitrova *et al.,* 1998) were transformed with the resulting plasmid pLexA-SynVipp1 as well as with the control plasmids. Growth of the cells and GALLEX measurements were done exactly as described in detail in Schneider and Engelman (2003).

RESULTS

Subcellular Localization of Vipp1 in Synechocystis

Vipp1 was found to bind to the inner envelope as well as to thylakoid membranes in chloroplasts from *Pisum sativum* and *A. thaliana* (Li *et al.*, 1994; Kroll *et al.*, 2001), whereas it has been proposed that in the cyanobacterium *Synechocystis* PCC 6803 Vipp1 is localized exclusively at the cytoplasmic membrane (Westphal *et al.*, 2001). Because chloroplasts and cyanobacteria share a common ancestor this different localization appeared surprising, thus we have revisited the subcellular localization of Vipp1 in *Synechocystis*. To visualize the subcellular localization of Vipp1 in *Synechocystis* cells, we have used EM together with immunogold labeling. As can be seen in Figure 1A the preimmune serum did not cross-react with any protein from *Synechocystis*, whereas the raised anti-Vipp1 serum showed a clear cross-reactivity with a single protein. Furthermore, when ultrathin sections of *Synechocystis* cells were also probed with the preimmune serum no gold particle was found on the EM micrographs (Figure 1B). Taken together, these control experiments clearly show that neither the preimmune serum nor the secondary antibodies cross-react unspecifically with any *Synechocystis* protein different from Vipp1. On the other hand, when ultrathin sections of *Synechocystis* cells were probed with the antibody directed against Vipp1 from *Synechocystis*, the protein was localized at different places within the entire *Synechocystis* cell (Figure 1C). Although most gold particles were found close to membranes, they were not exclusively localized in close proximity to the cytoplasmic membrane but also were close to thylakoid membranes within the cells, which is in good agreement with the described Vipp1 localization in *Pisum* and *Arabidopsis* chloroplasts. About two-third of all gold particles were found in close proximity to membranes, whereas one-third of the gold particles appeared to indicate a localization of (soluble) Vipp1 in the cytoplasm (n = 80). To further test if Vipp1 is exclusively membrane bound in *Synechocystis*, we have examined total cellular *Synechocystis* extract as well as isolated membranes and soluble *Synechocystis* proteins by Western blot analysis. As can be seen in Figure 1D, Vipp1 is mainly associated with membranes but also found in the soluble protein fraction, which indicates a dynamic equilibrium between membrane-bound and soluble Vipp1 in *Synechocystis*. However, in line with earlier reports the majority of Vipp1 was found to be membrane associated. In the soluble protein fraction a Vipp1 double band was detected by Western analyses, the exact nature of which is elusive. However, a Vipp1 double band has been described in most studies with Vipp1 so far (Kroll *et al.*, 2001; Aseeva *et al.*, 2004; Liu *et al.*, 2005), and this band most likely represents a proteolytic fragment of the full-length Vipp1. To further exclude that the observed fraction of soluble Vipp1 was not simply caused by the release of Vipp1 from membranes during isolation, we further analyzed *Synechocystis* cell growth under light-activated photoheterotrophic growth conditions, where growth does not depend on photosynthesis but solely on glucose (Anderson and McIntosh, 1991). Under these growth conditions *Synechocystis* cells contain only very few internal thylakoid membranes (Figure 1E). When ultrathin sections of *Synechocystis* cells grown under such conditions are analyzed with the anti-Vipp1 antibody (Figure 1E), we found a large fraction of Vipp1 not associated with any internal membranes, which further supports the above-mentioned observations with photoautotrophically grown cells.

Taken together, we conclude that, although a large fraction of Vipp1 is bound to membranes, the protein also exists
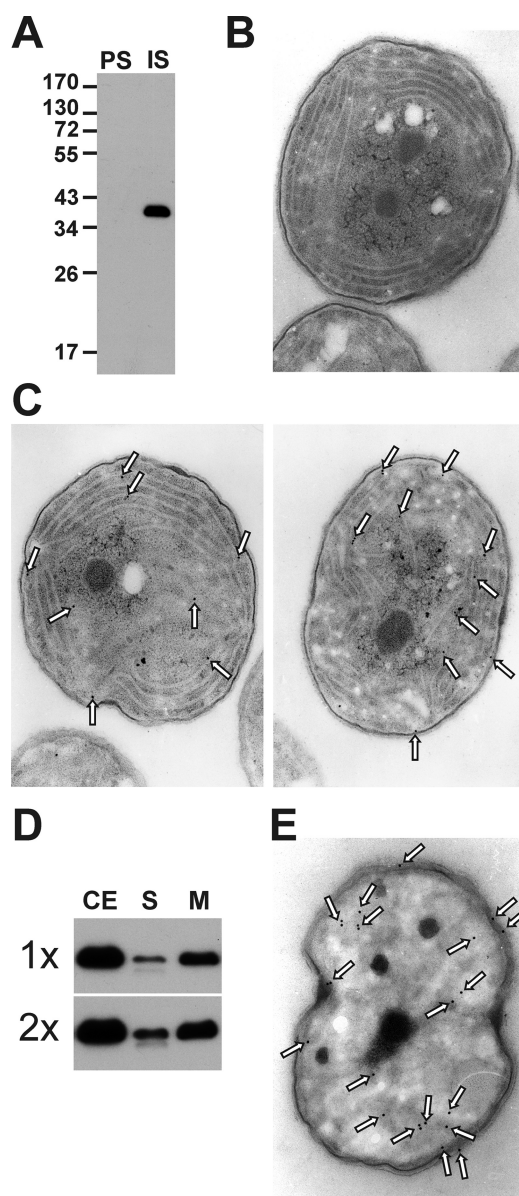

Figure 1. Subcellular localization of Vipp1 in *Synechocystis* PCC 6803. (A) Immunological analysis of *Synechocystis* cellular extracts (5 µg protein) with an anti-Vipp1 antiserum (IS) and the preimmune serum (PS). Only the anti-Vipp1 serum specifically recognized the Vipp1 protein. Although the calculated molecular mass of Vipp1 is 29 kDa, the apparent mass is ~38 kDa. The molecular masses of the standard proteins are indicated on the left. (B) As observed on Western blots, also no protein could be immunostained on electron micrographs with the preimmune serum and the secondary antibody. (C) Electron micrographs of *Synechocystis* cells immunostained with an anti-Vipp1 antiserum (dilution 1:100) followed by treatment with gold conjugated anti-rabbit IgG. The results indicate a preferential localization of Vipp1 in the vicinity of membranes. (D) Total cellular extract of *Synechocystis* (CE) as well as isolated membranes (M) and soluble proteins (S) were analyzed with an anti-Vipp1 antibody. The samples loaded to each lane corresponded to the same amount of cell material. Western blots with two different amounts of the individual fractions are shown to demonstrate that the loaded amounts of cellular extract, soluble proteins, and membranes are in a linear response range for each sample. (E) Electron micrographs of *Synechocystis* cell growth under light-activated heterotrophic growth conditions and immunostaining with an anti-Vipp1 antiserum (dilution 1:100) followed by treatment with gold-conjugated anti-rabbit IgG. The results indicate a localization of Vipp1 in the cytoplasm as well as close to membranes.
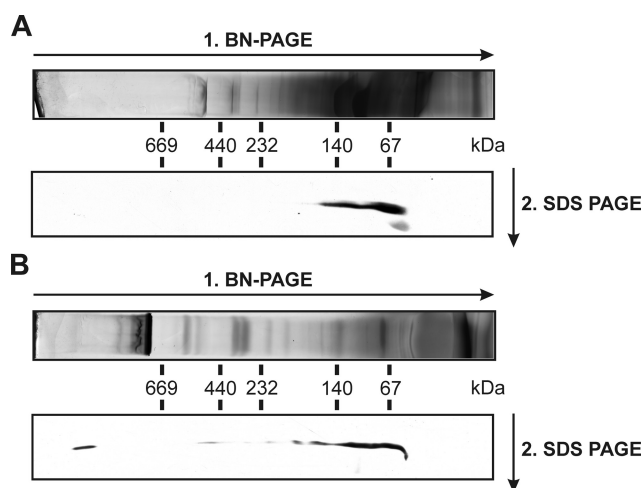
Figure 2. Two-dimensional BN/SDS-PAGE analysis of soluble (A) and membrane-bound (B) proteins and protein complexes from *Synechocystis*. Protein, 1 µg, was separated on a 4.5–16% BN-poly-acrylamide gel. Lanes of the BN-PAGE gel (shown on top) were subjected to SDS-PAGE (12% acrylamide) in the second dimension. After Western blotting Vipp1 was identified with an anti-Vipp1 antibody.

Figure 3. Analysis of soluble and membrane-bound proteins from *Synechocystis* by SEC. Membrane proteins were solubilized with 1.5% DDM and subsequently separated on a Biosept S4000 SEC column (Phenomenex). Identical volumes of individual SEC protein fractions were applied to a 12% SDS gel, and proteins were subsequently analyzed by Western blot analyses. In both the soluble and membrane-bound protein fraction Vipp1 was found as a dimer as well as an oligomer with a molecular mass of ~2 MDa.

in a soluble form in *Synechocystis*. The membrane-bound fraction is localized at the cytoplasmic as well as at the thylakoid membrane, in agreement with its described subcellular localization in chloroplasts.

Oligomerization of Vipp1 in Synechocystis

To analyze the oligomeric organization of Vipp1 from *Synechocystis* in more detail, we have separated soluble as well as membrane-bound and/or associated protein complexes and subsequently performed BN-PAGE and Western blot analyses. As can be seen in Figure 2, after separation of membrane-associated proteins and protein complexes a Vipp1 species with an apparent molecular mass of ~66 kDa was detected as well as a higher-ordered Vipp1 oligomer, which hardly entered the BN gel. These apparent molecular masses correspond to a Vipp1 dimer and a large Vipp1 oligomer with a high molecular mass (>1 MDa), although the exact mass cannot be resolved by BN-PAGE analysis. Interestingly, when soluble proteins from *Synechocystis* were analyzed by BN-PAGE, only the dimeric Vipp1 population was detected. Because this might indicate that the large Vipp1 oligomers form exclusively at membranes, we further analyzed the oligomeric state of Vipp1 by size exclusion chromatography (SEC). This milder technique more likely preserves oligomeric structures. In line with the BN-PAGE analysis a Vipp1 population with a molecular mass of ~66 kDa (dimer) as well as a large Vipp1 oligomer with masses ranging from 1.6 MDa to ~2 MDa were identified (Figure 3). In contrast to the BN-PAGE analysis, the higher-ordered Vipp1 oligomers were found in both the soluble as well as in the membrane protein fraction. These data indicate that Vipp1 forms higher-ordered oligomers in *Synechocystis,* and there may exist a dynamic equilibrium between monomers, dimers, and higher-ordered oligomers.

However, because the presented in vitro analyses were performed with protein fractions isolated from *Synechocystis* cells, the question arose if Vipp1 also forms oligomers within living cells. To test the oligomerization propensity of Vipp1 in a growing cell culture, we have used the GALLEX
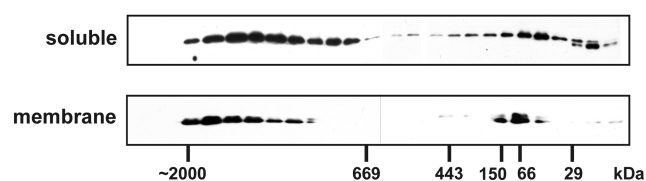
system (Schneider and Engelman, 2003). In this system a protein of interest is fused to the DNA-binding domain of the *E. coli* LexA protein. Oligomerization of a protein brings (at least) two LexA DNA-binding domains together, and only a dimeric LexA DNA-binding domain can properly bind to a promoter/operator region in the chromosome of an *E. coli* reporter strain. DNA binding subsequently represses the activity of a reporter gene expressing the β-galactosidase, and, thus, interaction of proteins can be followed by measuring the activity of the reporter. This LexA-based system has initially been used with soluble proteins (Dmitrova *et al.*, 1998; Daines and Silver, 2000) but has subsequently been modified for membrane localized proteins (Schneider and Engelman, 2004a,b; Prodöhl *et al.*, 2005, 2007). To evaluate the determined Vipp1 oligomerization propensities properly, we have also analyzed interaction of the transmembrane helix of the human glycophorin A (GpA) wild-type protein as well as of a mutated GpA helix carrying the G83I substitution, which significantly lowers the interaction propensity of the helix (Schneider and Engelman, 2003; Finger *et al.*, 2006).

The results of the GALLEX measurements are shown in Figure 4. Based on these results, Vipp1 forms stable oligomers in a living cell, and compared with GpA, which forms a stable helix dimer, Vipp1 has a rather strong oligomerization propensity. For all expressed chimeric proteins we found similar expression levels when tested with an anti-LexA antibody. It has to be noted at this stage, however, that although the GALLEX assay allows a meaningful description of a proteins general oligomerization propensity the measurement does not allow drawing any conclusion about the exact oligomeric state of the protein.

Taken together the above presented results strongly suggest that the *Synechocystis* Vipp1 forms stable oligomers with a mass of ~2 MDa that exist in vivo as nonbound and membrane-bound complexes.

Heterologous Expression of Vipp1

The above described measurements of Vipp1 oligomerization in *E. coli* cells have indicated that Vipp1 can be expressed as a stable oligomer in *E. coli*. Thus, to purify large amounts of the protein for further structural studies, we heterologously expressed the *Synechocystis* Vipp1 in *E. coli* cells. As can be seen in Figure 5, after expression of Vipp1 the protein was found to be mainly associated with membranes. Furthermore, as in *Synechocystis* a small pool of soluble Vipp1 was identified. To subsequently analyze these oligomeric structures in more detail, we have purified the protein from *E. coli* cell extracts (membranes and supernatant) without using any detergent or denaturant, because it has been suggested that the use of detergents can modify the
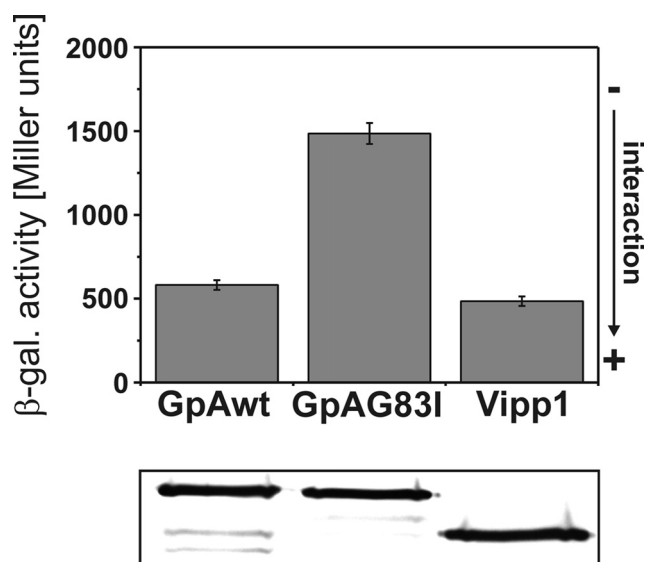
Figure 4. In vivo oligomerization of Vipp1. The propensity of Vipp1 to homooligomerize was measured with the GALLEX-system (Schneider and Engelman, 2003). As internal controls, the capacity of the wild-type and G83I-mutated GpA proteins to homo-dimerize was measured. The association capacity of each protein was determined by measuring the β-galactosidase activities of three independent clones. The expression level of the individual fusion proteins was tested by Western blot analysis using an anti-LexA antibody.

Figure 5. Top, expression of the *Synechocystis* Vipp1 in *E. coli*. Proteins were separated on a 12% SDS gel and stained with Coomassie blue. MW, molecular mass standard; CE, total cell extract of *E. coli* BL21 (DE3) cells harboring the expression plasmid pRSET-SynVipp1; IB, inclusion body fraction; S, soluble proteins; M, membrane proteins. Equal volumes of the individual *E. coli* fractions were loaded per lane. Vipp1, Vipp1 purified by affinity chromatography (1 μg). Bottom, an antibody was directed against Vipp1 cross-reacted with the purified Vipp1 and recognized Vipp1 in the individual *E. coli* fractions.

Vipp1 structure, resulting in nonnative structural alterations (Standar *et al.*, 2008). On purification we have analyzed the secondary structure of Vipp1 by CD spectroscopy. Computational analysis of the Vipp1 amino acid sequence with the program Jpred3 (Cole *et al.*, 2008) predicts that ~80% of the protein is α-helical, and many regions are predicted to have a high propensity to form coiled-coil structures (Figure 6A). The CD spectra of the purified *Synechocystis* Vipp1 is shown in Figure 6B and deconvolution of the spectra with the program CDSSTR (Compton and Johnson, 1986; Manavalan and Johnson, 1987; Sreerama and Woody, 2000; Whitmore and Wallace, 2004, 2008) predicts that 83% of Vipp1 is α-helical, which is in very good agreement with the computational prediction.

Interestingly, the ratio of the molar ellipticity at 222 nm to the molar ellipticity at 208 nm was found to be >1, which is indicative for formation of higher-ordered coiled coil structures (Monera *et al.*, 1993). Analyses of purified Vipp1 by BN-PAGE in combination with SEC (Figure 7) showed the same organization of Vipp1 into dimers and higher-ordered oligomers as has been observed before in *Synechocystis* cells (Figures 2 and 3).

Oligomeric Structure of Vipp1

To further investigate the structure of the Vipp1 oligomers, we have characterized the purified protein fraction by single particle EM analysis. As can be seen in Figure 8, Vipp1 forms large ring structures with different diameters between 25 and 33 nm. The Vipp1 ring structures are composed of distinct units each with a small protein density at the inside and a notable "spike" protruding from the outside (Figure 8A). The presence of the spikes facilitates an accurate determination of the rotational symmetry of the various types of rings. Interestingly, Vipp1 was found to form (at least) six
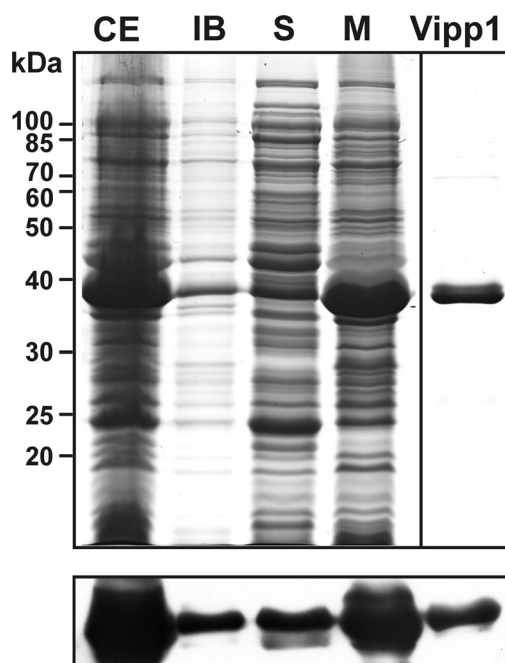
different types of rings with 12–17-fold rotational symmetry (Figure 8, B and C).

Occasionally, two Vipp1 rings become stacked. These double rings were only seen in side-view position (Figure 9D-H). The stacked double rings have a slight variation in diameter, which is between 29 and 34 nm (Figure 9, D–H, horizontal direction). This can be attributed to the above described variation in ring sizes. As expected, the height of the single rings (22 nm, half of the vertical direction) is uniform.

From its shape and dimensions, the mass of a protein complex can be roughly estimated. The 17-fold symmetrical ring has a volume of ~25,000 nm³, compatible with a mass of 1.5–2.5 MDa. A mass of ~2 MDa was also actually measured. Because the smallest building block of each ring is the Vipp1 monomer with a molecular mass of ~32 kDa and because the ring structures most likely consist of Vipp1 tetramers, rings with 12–17 tetrameric units would result in predicted masses of ~1500–2200 kDa. To further assess the nature of the Vipp1 building units shaping the various Vipp1 rings, we have analyzed Vipp1 oligomers by BN-PAGE after mild SDS denaturation of the Vipp1 rings. Addition of gradually increasing concentrations of SDS to Vipp1 dissolved in 5 mM DDM resulted in the formation of mixed DDM/SDS micelles and gradual disassembly of the Vipp1 oligomers.

At SDS concentrations above 4 mM the large oligomer disappears, whereas dimeric and tetrameric Vipp1 species appear, as well as a small fraction of octameric Vipp1 (Figure 10). At increasing SDS concentrations the higher-ordered oligomers disassemble completely, and only the dimeric
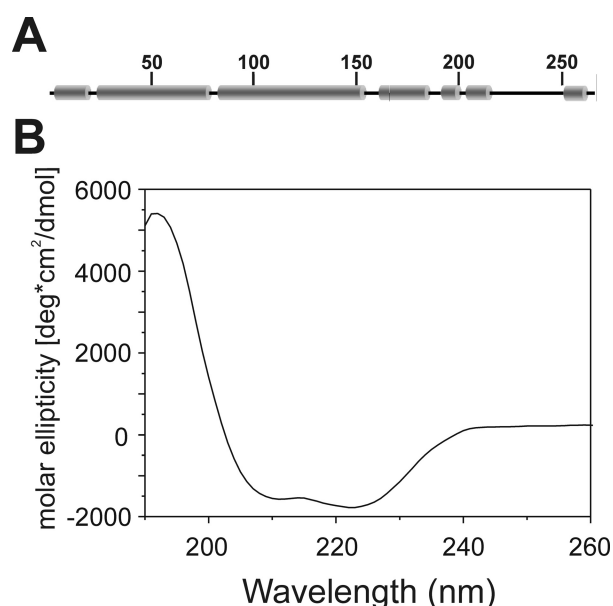
Figure 6. Analysis of the Vipp1 secondary structure. (A) Analysis of the Vipp1 amino acid sequence with the program Jpred3 (Cole *et al.*, 2008) predicts that ~80% of Vipp1 is α-helical. The α-helical protein regions are indicated by the bars. (B) CD spectra of the isolated Vipp1 in the range between 190 and 260 nm. Deconvolution of the CD spectra predicts that 83% of Vipp1 is α-helical. Note that the ratio of the ellipticities at 222 and 208 nm is >1. For further details see the text.

Vipp1 remains stable. Thus, in line with the above presented observations Vipp1 forms stable dimers in solution. Therefore, we propose that the repeating unit for a Vipp1 ring is a dimer of Vipp1 dimers. This implies, e.g., for the ring with N = 12 spikes that 24 Vipp1 dimers are involved in formation of the oligomer, with each spike representing a dimer. However, because the spikes facing inside the protein have an electron density different that of the spikes facing to the outside, we suggest that the Vipp1 oligomer is built up by an alternating interaction of Vipp1 dimers, potentially in an antiparallel manner. The side views of the Vipp1 rings indicate that there is no clear separation within distinct domains in the vertical direction (Figure 9, D–H). Because the rings have a height of ~22 nm, this means that more than half of the Vipp1 monomer must exist in an extended α-helical conformation, spanning the entire height of the complex, which is 22 nm.
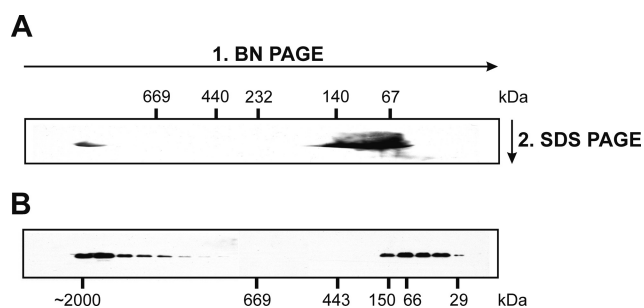

Figure 7. Characterization of the isolated Vipp1. When analyzed by BN-PAGE (A) and SEC (B), the isolated Vipp1 shows an identical pattern of dimers and higher-ordered oligomers as observed in *Synechocystis* cellular extracts (cf. Figures 2–4).

In addition to the observed ring structures, a few string-like open ring structures were found (Figure 9, A–C), and, in addition, a very small part of the entire population of Vipp1 rings was found to form longer rods (Figure 9I).

Taken together, the presented results show that Vipp1 from *Synechocystis* can form ring structures with different diameters but constant heights, and dimeric Vipp1 is the minimal building block involved in formation of the observed higher-ordered oligomeric structures.

DISCUSSION

Subcellular Localization of Vipp1

In the present study we have analyzed the subcellular localization and structural organization of Vipp1 from the cyanobacterium *Synechocystis* sp. PCC 6803. For Vipp1 from *A. thaliana, Pisum sativum,* and *Synechocystis*, it has been suggested that the proteins are exclusively membrane bound (Li *et al.*, 1994; Kroll *et al.*, 2001; Westphal *et al.*, 2001). Although for the chloroplast Vipp1 a dual localization at both the inner envelope membrane as well as at the thylakoid membrane has been described (Kroll *et al.*, 2001), for *Synechocystis* it has been suggested that the protein binds exclusively to the cytoplasmic membrane and not to thylakoids (Westphal *et al.*, 2001). This observation was somewhat unexpected because of the common evolutionary origin of cyanobacteria and chloroplasts and of the proposed function of the protein. If Vipp1 is involved in a vesicular transfer system between the inner membrane systems in chloroplasts and cyanobacteria, one would expect to find the protein localized at both inner membranes as in chloroplasts. In line with the described subcellular localization in chloroplasts the immunogold analysis presented in Figure 1 strongly suggest that cyanobacterial Vipp1 is also attached to both the cytoplasmic and the thylakoid membrane. Thus, in cyanobacteria the protein could be involved in an interlinked communication between the two internal membrane systems as well. However, in contrast to earlier observation a fraction of soluble, non-bound Vipp1 was also identified in *Synechocystis*. Thus, although the majority of Vipp1 appears to be tightly attached to membranes in *Synechocystis*, a soluble protein population is also present, and, as the membrane-bound fraction, soluble Vipp1 also forms higher-ordered oligomers. This observation is in excellent agreement with observations described earlier for PspA from *E. coli*. In *E. coli* PspA exists in a soluble and in a membrane-bound form (Brissette *et al.*, 1990), and a dynamic equilibrium between these two stages is suggested to trigger the activity of the protein (Elderkin *et al.*, 2002; Hankamer *et al.*, 2004). However, it is also possible that cytoplasmic oligomerization of Vipp1 is just a maturation step before membrane binding or even a prerequisite for this.

Structural Organization of Vipp1

Analysis of soluble as well as membrane-bound proteins from *Synechocystis* by BN-PAGE indicates that in *Synechocystis* Vipp1 exists as a stable dimer as well as oligomers with a molecular mass of ≫1 MDa. Thus, the protein appears to form larger oligomers than its homologue PspA from *E. coli*. Interestingly, our BN-PAGE analyses indicated that the oligomers were present only in the membrane protein fraction and not in the soluble protein fraction, which indicates that the membrane-bound oligomer is more stable than the soluble one. To further characterize the oligomeric organization of the *Synechocystis* Vipp1, we have subsequently analyzed
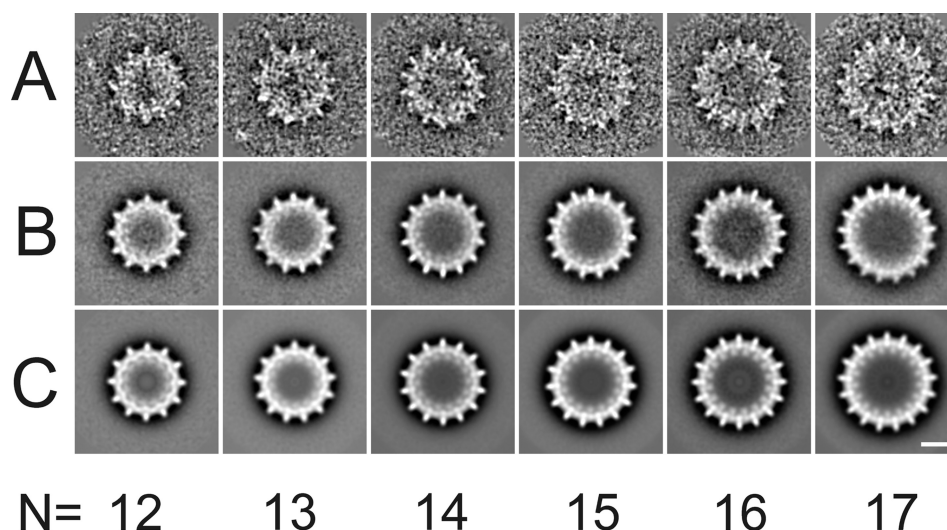
Figure 8. Single-particle image analysis and classification of a set of 15,000 Vipp1 rings. (A) A gallery of single-particle projections in top-view position. (B) Class-sums of nonsymmetrized projection maps of rings with different rotational symmetry. On average, for each projection map ~200–300 projections were summed. (C) Same rings corresponding to the frames of B, with imposed rotational symmetries. Space bar, 10 nm.

the protein organization by SEC, and dimeric Vipp1 as well as a Vipp1 population with a significantly higher molecular mass was identified in the soluble as well as in the membrane-bound protein fractions from *Synechocystis*. The molecular mass of the larger oligomer was estimated to be ~2 MDa. Formation of rod-like structures with molecular masses ≫2 MDa, as described in Liu *et al.*, (2007), was not observed, and, thus, the described results strongly suggest that—at least the *Synechocystis*—Vipp1 does not form larger oligomeric assemblies.

After expression of the *Synechocystis* Vipp1 in *E. coli* the monomeric protein strongly interacts and forms higher-ordered oligomers (Figures 5 and 7). Analysis of the purified protein by SEC demonstrated that also the isolated protein forms large oligomeric structures with a molecular mass of ~2 MDa, as observed in *Synechocystis* before. Because an impact of detergent on the structural organization of PspA

from *E. coli* has been emphasized (Standar *et al.*, 2008), it has to be mentioned that the protein was purified without any detergent. Because the protein can be well purified and, thus, effectively washed off the membranes by this method, this observation may indicate that Vipp1 is not very tightly bound to the internal membranes, at least not in *E. coli*. This might be caused by the different lipid composition of the *E. coli* membranes compared with the *Synechocystis* membranes. However, as also the homologous protein PspA from *E. coli* was purified by a similar method after homologous expression this protein appears also not to bind tightly to membranes (Standar *et al.*, 2008). Weak membrane
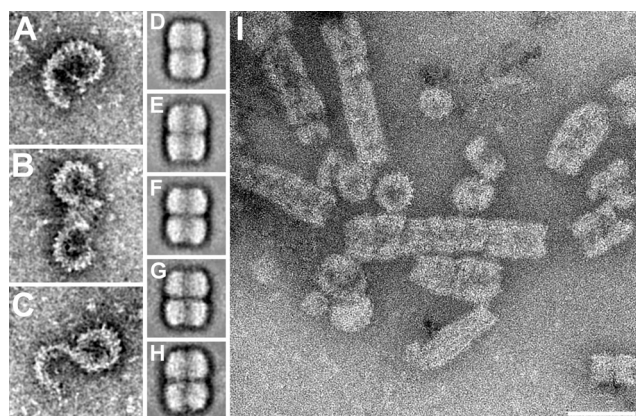

Figure 9. EM nonfrequent types of Vipp1 structures. (A–C) open rings formed by Vipp1. (D–H) Classification of sandwiched Vipp1 rings in side-view position. For each class-sum ~50–100 projections were summed. (I) Overview of rarely occurring rod-like association of Vipp1 rings. In the middle of the frame some individual rings are visible. Space bar for all frames, 50 nm.
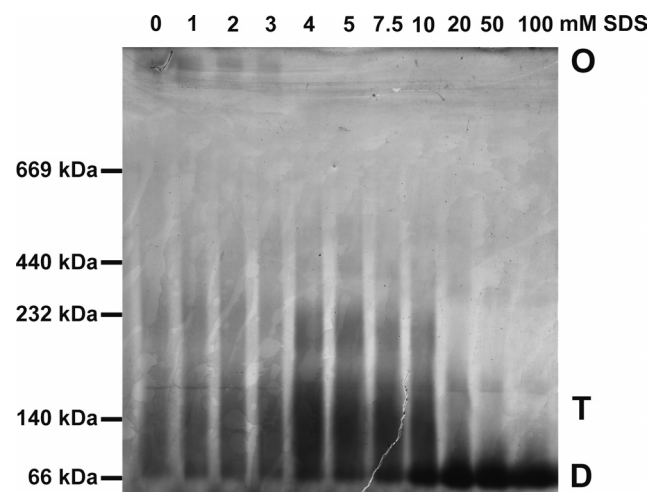

Figure 10. Gradual disassembly of the ~2 MDa Vipp1 oligomer. Vipp1 was dissolved in buffer in the presence of 5 mM DDM, and the indicated amounts of SDS were added to form mixed micelles. After incubation at room temperature for 10 min, protein complexes were separated on a 4.5–16% BN polyacrylamide gel, and the gel was subsequently silver-stained. The positions of the Vipp1 dimer (D), the tetramer (T), and of higher organized oligomers (O) are indicated.

attachment could thus be a common feature of PspA/Vipp1 proteins.

EM shows that Vipp1 monomers can form various higher-ordered structures, and the BN-PAGE analysis shown in Figure 10 suggests that the these structures are build up by accumulation of multiple dimeric Vipp1 species. Numerous Vipp1 proteins laterally associate to form small strings (Figure 9, A–C), which eventually close to form Vipp1 rings. The strings shown in Figure 9, A–C, could either represent assembly intermediates or an early step during Vipp1 ring degradation. In either case the strings clearly indicate an organization of Vipp1 by lateral accumulation of multiple monomers. Occasionally, two Vipp1 rings can further interact to form a double-ring structure (Figure 9, D–H). It is appealing to speculate that both Vipp1 rings interact with a rather hydrophobic surface, which is otherwise involved in membrane binding. Single-particle EM analysis of purified Vipp1 showed formation of various homooligomeric Vipp1 ring structures with different diameters. Actually, Vipp1 is to our knowledge rather special to make such a variety of rings, which means that there must be a special function linked to it, as will be discussed below. A similar diversity of ring structure with different compositions of the building units has—to our knowledge—only been described so far for the IsiA complex from *Synechocystis* (Boekema *et al.*, 2001; Kouril *et al.*, 2003, 2005; Yeremenko *et al.*, 2004).

It is also interesting to compare the Vipp1 rings with those of the structural and functional homologous PspA protein. The Vipp1 rings have a 12–17-fold symmetry and a diameter of 25–33 nm, whereas the PspA rings are uniform with a ninefold symmetrical configuration (Hankamer *et al.*, 2004). If we extrapolate to a hypothetical Vipp1 ring with ninefold symmetry, this ring would have a diameter of 22 nm. This is close to the actual PspA ring diameter of 20 nm, if we take into account that the latter ring has a rather smooth surface because it lacks spikes like Vipp1 has. The PspA rings were considered to be composed of tetrameric building blocks to form uniform rings with a molecular mass of ~1 MDa (Hankamer *et al.*, 2004). This equals the size of half of the Vipp1 rings, which can be explained by the fact that the ring height is only 8.5 nm. This difference in the height of the PspA rings versus the Vipp1 rings indicates that packing of the PspA and Vipp1 monomers in the two rings must be different. Although Vipp1 is C-terminally prolonged when compared with PspA, oligomerization of the Vipp1 monomers depends only on the PspA-like N-terminal domains (Aseeva *et al.*, 2004). Thus, the C-terminal extension of Vipp1 is most likely not directly involved in formation of the ring structures. Because of this, the N-terminal core domain of PspA and Vipp1 must pack differently. Although only ~25% of the PspA amino acid residues must form an extended α-helix to span the height of the PspA ring (8 nm), ~50% of Vipp1 has to form an extended α-helix to span 22 nm. For both proteins a domain of ~140 amino acids of the N-terminal region is predicted to form an α-helix with a high propensity for coiled-coil formation. For Vipp1 this predicted α-helical domain of 140 amino acids would have the right length to account for the determined height of the rings of 22 nm, if present as one giant extended α-helix. In the case of PspA this helix is most likely folded as a hairpin and may form an α-helix bundle that would result in an increase of the PspA ring width. Different structural organization of PspA and Vipp1 might also indicate small differences in the respective protein functions, which would, e.g., explain why *Synechocystis* contains PspA as well as Vipp1.

It has to be noted that we did not observe cage-like structures as described before for the PspA from *E. coli*. Because for the preparation of the *Synechocystis* Vipp1 no detergent was used the suggested major impact of detergent on the PspA structure (ring vs. cage structures) should be revisited.

The observed diverse ring structures of Vipp1 could be involved in vesicle formation in cyanobacteria and chloroplasts. It is intriguing to speculate that Vipp1 assembled into a ring around the neck of a forming budding vesicle, similar to dynamin in eukaryotic cells.

Stepwise release of individual Vipp1 units results in formation of rings with smaller diameters, which would bring the membranes into a close contact, resulting in membrane fusion and pitching off of a vesicle. If Vipp1 performs such a dynamin-like function, the protein will most likely recruit other proteins that are, for example, involved in initial membrane bending and vesicle fission. Proteins involved in regulating the controlled Vipp1 (dis)assembly could involve Hsp70 chaperones and cochaperones, as discussed recently (Liu *et al.*, 2007).

Taken together, we show here that *Synechocystis* Vipp1 forms various oligomeric rings with different monomer stoichiometries. Although some of these rings exist in the cytoplasm of *Synechocystis* in a soluble form, most Vipp1 oligomers are tightly attached to both the thylakoid and the cytoplasmic membrane of the cyanobacterium *Synechocystis* sp. PCC 6803. Formation of promiscuous Vipp1 ring structures could play a critical role in vesicle formation in cyanobacteria and chloroplasts.

REFERENCES

Anderson, S. L., and McIntosh, L. (1991). Light-activated heterotrophic growth of the cyanobacterium *Synechocystis* sp. strain PCC *6803*, a blue-light-requiring process. J. Bacteriol. *173*, 2761–2767.

Aseeva, E., Ossenbühl, F., Eichacker, L. A., Wanner, G., Soll, J., and Vothknecht, U. C. (2004). Complex formation of Vipp1 depends on its alpha-helical PspA-like domain. J. Biol. Chem. *279*, 35535–35541.

Aseeva, E., *et al.* (2007). Vipp1 is required for basic thylakoid membrane formation but not for the assembly of thylakoid protein complexes. Plant Physiol. Biochem. *45*, 119–128.

Boekema, E. J., Hifney, A., Yakushevska, A. E., Piotrowski, M., Keegstra, W., Berry, S., Michel, K.-P., Pistorius, E. K., and Kruip, J. (2001). A giant chlorophyll-protein complex induced by iron deficiency in cyanobacteria. *412*, 745–748.

Brissette, J. L., Russel, M., Weiner, L., and Model, P. (1990). Phage shock protein, a stress protein of *Escherichia coli*. Proc. Natl. Acad. Sci. USA *87*, 862–866.

Cole, C., Barber, J. D., and Barton, G. J. (2008). The Jpred 3 secondary structure prediction server. Nucleic Acids Res. *36*, W197–W201.

Compton, L. A., and Johnson, W. C., Jr. (1986). Analysis of protein circular dichroism spectra for secondary structure using a simple matrix multiplication. Anal. Biochem. *155*, 155–167.

Daines, D. A., and Silver, R. P. (2000). Evidence for multimerization of neu proteins involved in polysialic acid synthesis in *Escherichia coli* K1 using improved LexA-based vectors. J. Bacteriol. *182*, 5267–5270.

DeLisa, M. P., Lee, P., Palmer, T., and Georgiou, G. (2004). Phage shock protein PspA of *Escherichia coli* relieves saturation of protein export via the Tat pathway. J. Bacteriol. *186*, 366–373.

Dmitrova, M., Younes-Cauet, G., Oertel-Buchheit, P., Porte, D., Schnarr, M., and Granger-Schnarr, M. (1998). A new LexA-based genetic system for monitoring and analyzing protein heterodimerization in *Escherichia coli*. Mol. Gen. Genet. *257*, 205–212.

Dühring, U., Irrgang, K. D., Lunser, K., Kehr, J., and Wilde, A. (2006). Analysis of photosynthetic complexes from a cyanobacterial ycf37 mutant. Biochim. Biophys. Acta *1757*, 3–11.

Elderkin, S., Jones, S., Schumacher, J., Studholme, D., and Buck, M. (2002). Mechanism of action of the *Escherichia coli* phage shock protein PspA in repression of the AAA family transcription factor PspF. J. Mol. Biol. *320*, 23–37.

Finger, C., Volkmer, T., Prodöhl, A., Otzen, D. E., Engelman, D. M., and Schneider, D. (2006). The stability of transmembrane helix interactions measured in a biological membrane. J. Mol. Biol. *358*, 1221–1228.

Fuhrmann, E., Gathmann, S., Rupprecht, E., Golecki, J., and Schneider, D. (2009). Thylakoid membrane reduction affects the photosystem stoichiometry in the cyanobacterium *Synechocystis* sp. PCC 6803. Plant Physiol. *149*, 735–744.

Gathmann, S., Rupprecht, E., Kahmann, U., and Schneider, D. (2008). A conserved structure and function of the YidC homologous protein Slr1471 from *Synechocystis* sp. PCC 6803. J. Microbiol. Biotechnol. *18*, 1090–1094.

Hankamer, B. D., Elderkin, S. L., Buck, M., and Nield, J. (2004). Organization of the AAA(+) adaptor protein PspA is an oligomeric ring. J. Biol. Chem. *279*, 8862–8866.

Kouril, R., Yeremenko, N., D'Haene, S., Oostergetel, G. T., Matthijs, H.C.P., Dekker, J. P., and Boekema, E. J. (2005). Supercomplexes of IsiA and Photosystem I in a mutant lacking subunit PsaL. Biochim. Biophys. Acta Bioenergetics *1706*, 262–266.

Kouril, R., Yeremenko, N., D'Haene, S., Yakushevska, A. E., Keegstra, W., Matthijs, H.C.P., Dekker, J. P., and Boekema, E. J. (2003). Photosystem I trimers from *Synechocystis* PCC 6803 lacking the PsaF and PsaJ subunits bind an IsiA ring of 17 units. Biochim. Biophys. Acta Bioenergetics *1607*, 1–4.

Kroll, D., Meierhoff, K., Bechtold, N., Kinoshita, M., Westphal, S., Vothknecht, U. C., Soll, J., and Westhoff, P. (2001). VIPP1, a nuclear gene of *Arabidopsis thaliana* essential for thylakoid membrane formation. Proc. Natl. Acad. Sci. USA *98*, 4238–4242.

Laemmli, U. K. (1970). Cleavage of structural proteins during the assembly of the head of bacteriophage T4. Nature *227*, 680–685.

Li, H. M., Kaneko, Y., and Keegstra, K. (1994). Molecular cloning of a chloroplastic protein associated with both the envelope and thylakoid membranes. Plant Mol. Biol. *25*, 619–632.

Liberton, M., Howard Berg, R., Heuser, J., Roth, R., and Pakrasi, H. B. (2006). Ultrastructure of the membrane systems in the unicellular cyanobacterium *Synechocystis* sp. strain PCC 6803. Protoplasma *227*, 129–138.

Liu, C., Willmund, F., Golecki, J. R., Cacace, S., Hess, B., Markert, C., and Schroda, M. (2007). The chloroplast HSP70B-CDJ2-CGE1 chaperones catalyse assembly and disassembly of VIPP1 oligomers in *Chlamydomonas.* Plant J. *50*, 265–277.

Liu, C., Willmund, F., Whitelegge, J. P., Hawat, S., Knapp, B., Lodha, M., and Schroda, M. (2005). J-domain protein CDJ2 and HSP70B are a plastidic chaperone pair that interacts with vesicle-inducing protein in plastids 1. Mol. Biol. Cell *16*, 1165–1177.

Manavalan, P., and Johnson, W. C., Jr. (1987). Variable selection method improves the prediction of protein secondary structure from circular dichroism spectra. Anal. Biochem. *167*, 76–85.

Monera, O., Zhou, N., Kay, C., and Hodges, R. (1993). Comparison of antiparallel and parallel two-stranded alpha-helical coiled-coils. Design, synthesis, and characterization. J. Biol. Chem. *268*, 19218–19227.

Nevo, R., Charuvi, D., Shimoni, E., Schwarz, R., Kaplan, A., Ohad, I., and Reich, Z. (2007). Thylakoid membrane perforations and connectivity enable intracellular traffic in cyanobacteria. EMBO J. *26*, 1467–1473.

Oostergetel, G. T., Keegstra, W., and Brisson, A. (1998). Automation of specimen selection and data acquisition for protein electron crystallography. Ultramicroscopy *74*, 47–59.

Prodöhl, A., Volkmer, T., Finger, C., and Schneider, D. (2005). Defining the structural basis for assembly of a transmembrane cytochrome. J. Mol. Biol. *350*, 744–756.

Prodöhl, A., Weber, M., Dreher, C., and Schneider, D. (2007). A mutational study of transmembrane helix-helix interactions. Biochimie *89*, 1433–1437.

Rippka, R., Deruelles, J., Waterbury, J. B., Herdman, M., and Stanier, R. Y. (1979). Pi-by-no assignments, strains histories and properties of pure cultures of cyanobacteria. J. Gen. Microbiol. *111*, 1–61.

Schneider, D., and Engelman, D. M. (2003). GALLEX, a measurement of heterologous association of transmembrane helices in a biological membrane. J. Biol. Chem. *278*, 3105–3111.

Schneider, D., and Engelman, D. M. (2004a). Involvement of transmembrane domain interactions in signal transduction by a/b Integrins. J. Biol. Chem. *279*, 9840–9846.

Schneider, D., and Engelman, D. M. (2004b). Motifs of two small residues can assist but are not sufficient to mediate transmembrane helix interactions J. Mol. Biol. *343*, 799–804.

Schneider, D., Fuhrmann, E., Scholz, I., Hess, W. R., and Graumann, P. L. (2007). Fluorescence staining of live cyanobacterial cells suggest non-stringent chromosome segregation and absence of a connection between cytoplasmic and thylakoid membranes. BMC Cell Biol. *8*, 39.

Sreerama, N., and Woody, R. W. (2000). Estimation of protein secondary structure from circular dichroism spectra: comparison of CONTIN, SELCON, and CDSSTR methods with an expanded reference set. Anal. Biochem. *287*, 252–260.

Standar, K., Mehner, D., Osadnik, H., Berthelmann, F., Hause, G., Lünsdorf, H., and Brüser, T. (2008). PspA can form large scaffolds in *Escherichia coli.* FEBS Lett. *582*, 3585–3589.

van de Meene, A. M., Hohmann-Marriott, M. F., Vermaas, W. F., and Roberson, R. W. (2006). The three-dimensional structure of the cyanobacterium *Synechocystis* sp. PCC 6803. Arch. Microbiol. *184*, 259–270.

van Heel, M., *et al.* (2000). Single-particle electron cryo-microscopy: towards atomic resolution. Quart. Rev. Biophys. *33*, 307–369.

Vothknecht, U. C., and Westhoff, P. (2001). Biogenesis and origin of thylakoid membranes. Biochim. Biophys. Acta *1541*, 91–101.

Westphal, S., Heins, L., Soll, J., and Vothknecht, U. C. (2001). Vipp1 deletion mutant of *Synechocystis*: a connection between bacterial phage shock and thylakoid biogenesis? Proc. Natl. Acad. Sci. USA *98*, 4243–4248.

Whitmore, L., and Wallace, B. A. (2004). DICHROWEB, an online server for protein secondary structure analyses from circular dichroism spectroscopic data. Nucleic Acids Res. *32*, W668–W673.

Whitmore, L., and Wallace, B. A. (2008). Protein secondary structure analyses from circular dichroism spectroscopy: methods and reference databases. Biopolymers *89*, 392–400.

Yeremenko, N., *et al.* (2004). Supramolecular organization and dual function of the IsiA chlorophyll-binding protein in cyanobacteria. Biochemistry *43*, 10308–10313.